Cell

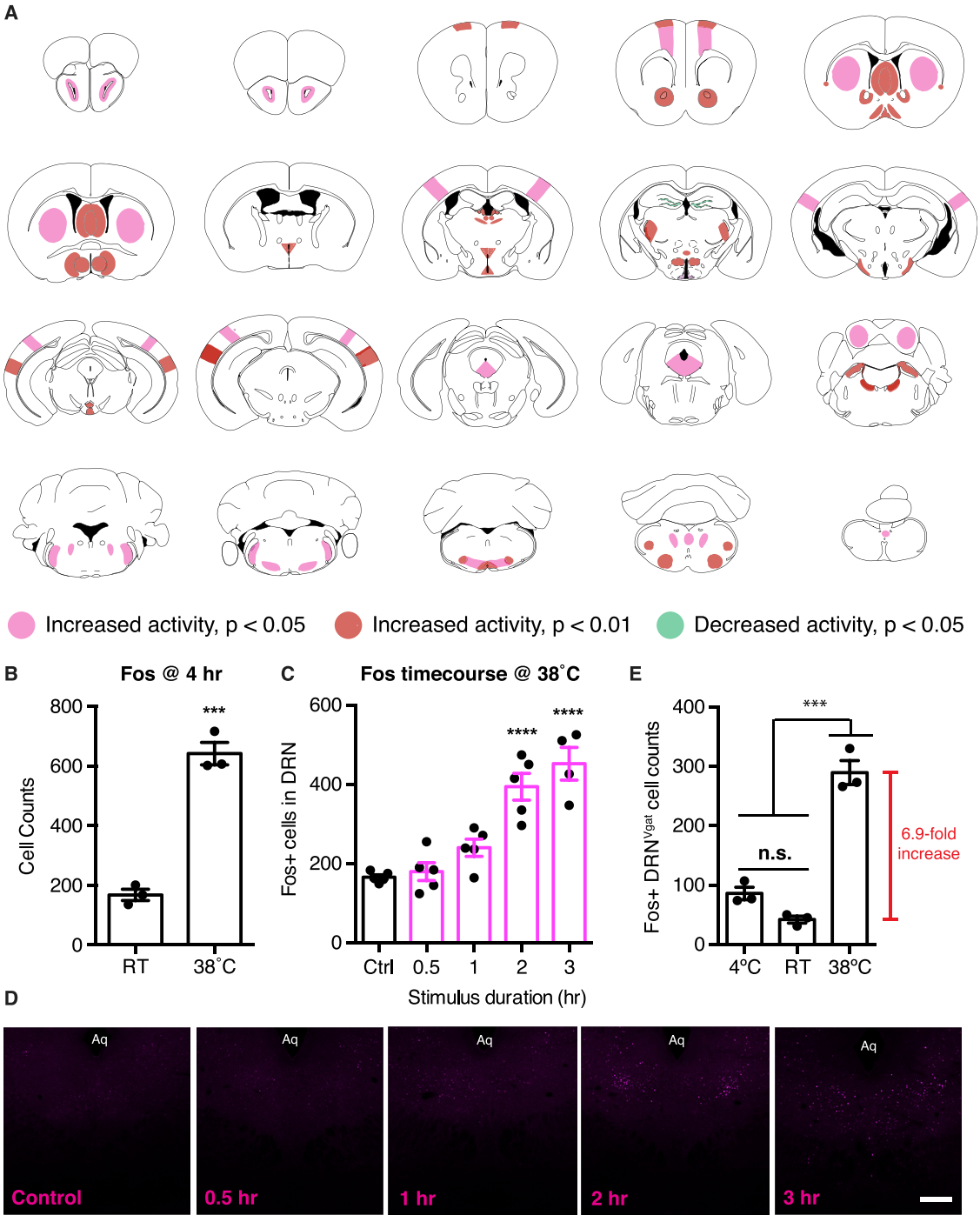

Figure S1. DRN^{Vgat} Neurons Are Activated by Ambient Warmth and Communicate Polysynaptically with iBAT, Related to Figure 1

(A) Graphical depiction of whole-brain activity mapping results for identifying novel loci activated by ambient heat challenge. Regions of both increased and decreased activity are shown.

(B) Fos expression is significantly increased in the DRN after 4 hr exposure to 38°C, as compared to RT ($p < 0.001$). Unpaired t test comparing RT and 38°C (n = 3 mice per group).

(C-D) Time course study for investigating Fos activation in the DRN for 0.5-3 hr exposure to 38°C. (C) Cell counts for time course study (taken from image sets represented in panel D); significant Fos counts were observed after 2+ hours of exposure to ambient warmth. (D) IHC results from Fos time course study.

(E) Absolute changes in DRN^{Vgat} neurons expressing Fos in response to different ambient temperatures (cold, room temperature, warm). One-way ANOVA comparing across treatments (Treatment: $p < 0.0001$).

Scale bar, 250 μm. ***$p < 0.001$, ****$p < 0.0001$. Data are presented as mean ± SEM.

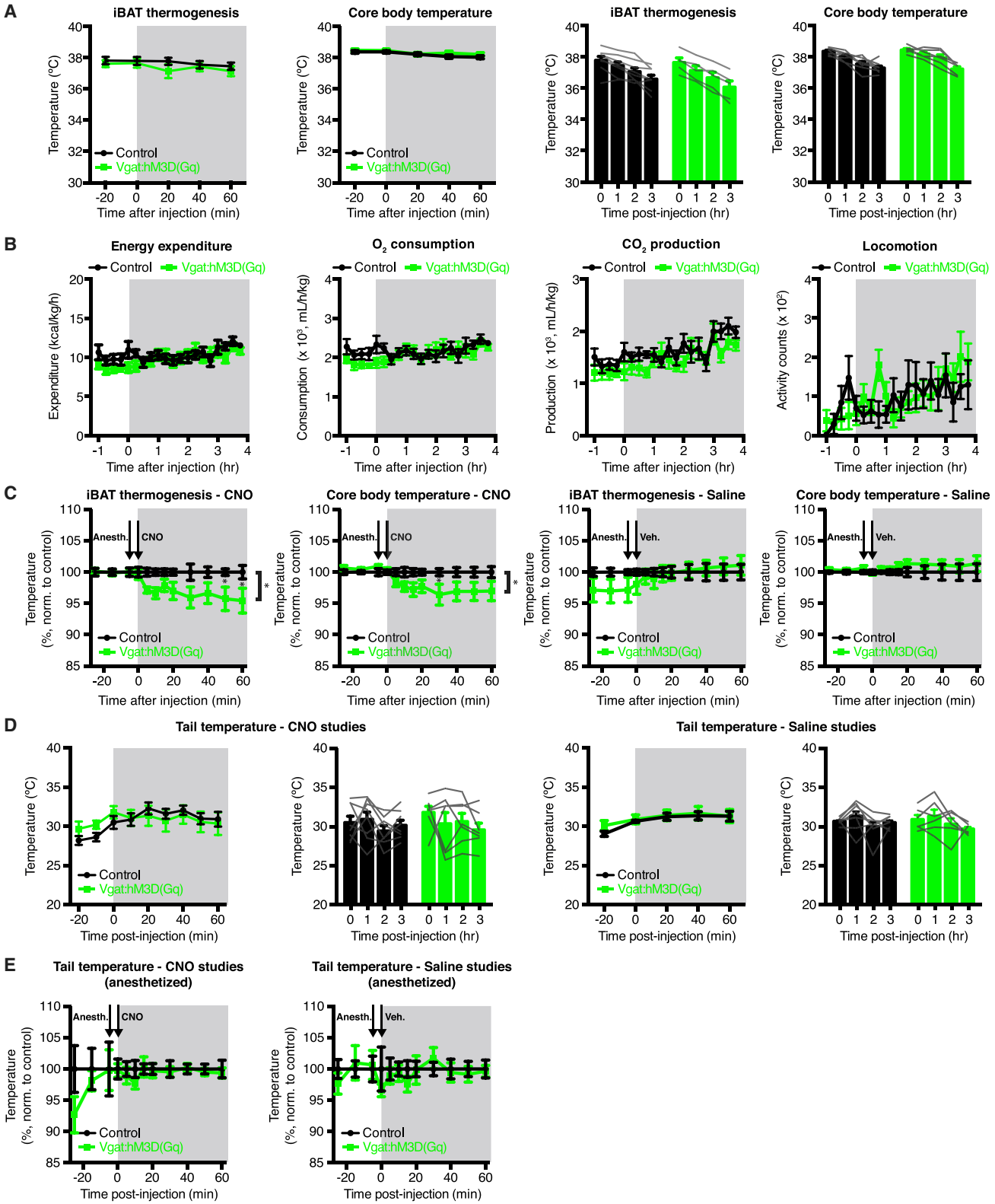

Figure S2. Control Studies for DRN^{Vgat} Neuron Activation, Related to Figure 2

(A) iBAT temperature (from implanted probes) and core (anal) temperature after i.p. injection of vehicle (saline). Injection of vehicle has no effect on iBAT or core temperature (Treatment: $p > 0.05$). Two-way RM-ANOVA comparing control and treated groups (n = 7-8 mice per group).

(legend continued on next page)

(B) Injection of vehicle has no effect on energy expenditure, oxygen consumption, carbon dioxide production, or locomotor activity (Treatment: $p > 0.05$ for all parameters). Two-way RM ANOVA comparing control and treated groups (n = 7-8 mice per group).

(C) iBAT temperature (from implanted probes) and core (anal) temperature after i.p. injection of CNO (left) or vehicle (right) during sedation (anesthetized preparation). Injection of CNO during sedation significantly suppresses both iBAT (Treatment: $p < 0.05$) and core temperature (Treatment: $p < 0.05$), whereas injection of vehicle (saline) during sedation has no effect on iBAT (Treatment: $p > 0.05$) or core temperature (Treatment: $p > 0.05$). Two-way RM-ANOVA comparing control and treated groups (n = 7-8 mice per group).

(D-E) Tail temperature (from thermal imaging) is not affected by CNO or vehicle (saline) injection under awake (D) or anesthetized preparations (E) (Treatment: $p > 0.05$ for all conditions). Two-way RM-ANOVA comparing control and treated groups (n = 7-8 mice per group).

*$p < 0.05$. Data are presented as mean ± SEM.

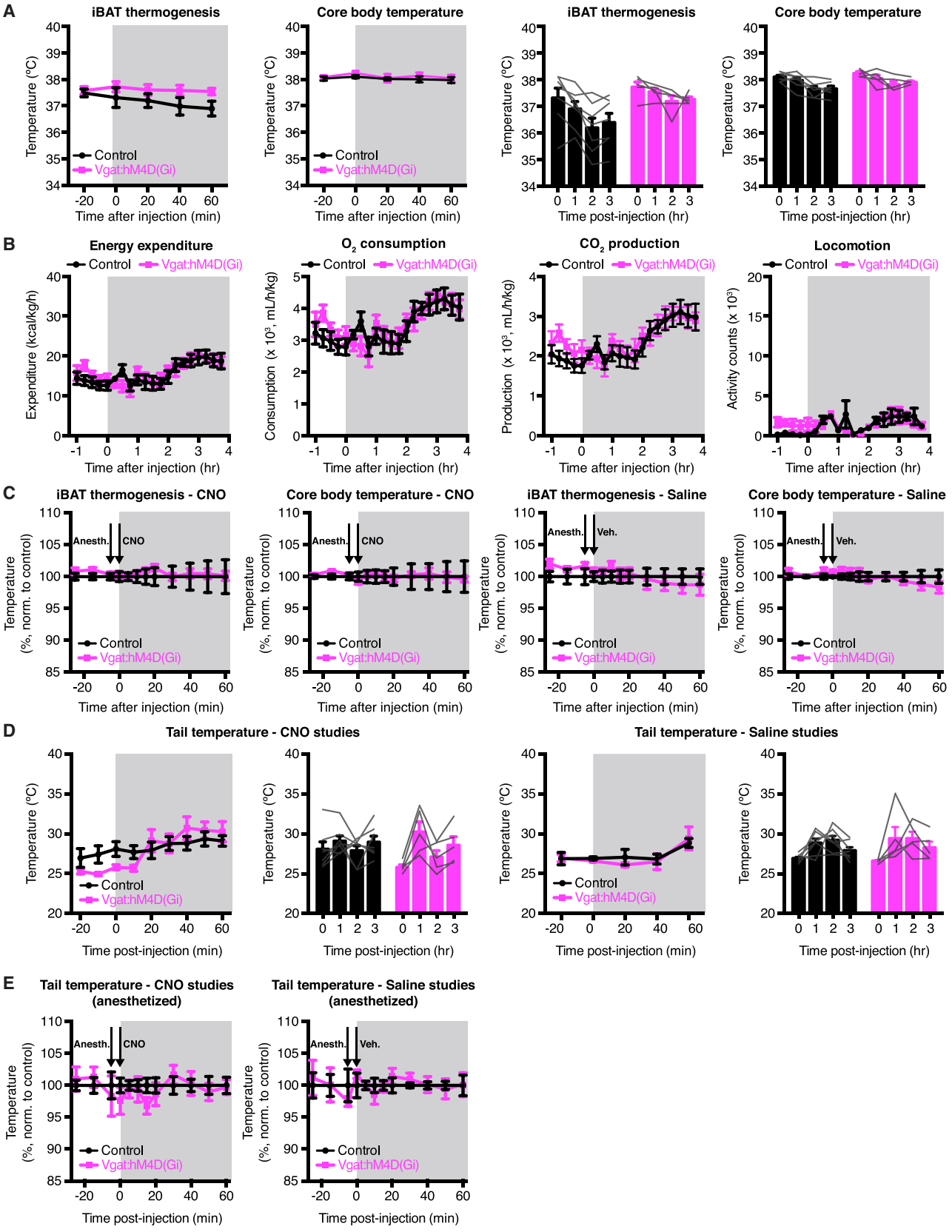

(legend on next page)

Figure S3. Control Studies for DRN^{Vgat} Neuron Inhibition, Related to Figure 3

(A) Quantification of iBAT temperature from thermal imaging and core (anal) temperature after i.p. injection of vehicle (saline). Injection of vehicle has no effect on iBAT or core temperature (Treatment: $p > 0.05$). Two-way RM-ANOVA comparing control and treated groups (n = 5-7 mice per group)

(B) Injection of vehicle has no effect on energy expenditure, oxygen consumption, carbon dioxide production, or locomotor activity (Treatment: $p > 0.05$ for all parameters). Two-way RM ANOVA comparing control and treated groups (n = 7 mice per group).

(C) iBAT temperature (from implanted probes) and core (anal) temperature after i.p. injection of CNO (left) or vehicle (right) during sedation (anesthetized preparation). Injection of CNO during sedation has no effect on iBAT (Treatment: $p > 0.05$) or core temperature (Treatment: $p > 0.05$); injection of vehicle (saline) during sedation also has no effect on iBAT (Treatment: $p > 0.05$) or core temperature (Treatment: $p > 0.05$). Two-way RM-ANOVA comparing control and treated groups (n = 5-7 mice per group).

(D-E) Tail temperature (from thermal imaging) is not affected by CNO or vehicle (saline) injection under awake (D) or anesthetized preparations (E) (Treatment: $p > 0.05$ for all conditions). Two-way RM-ANOVA comparing control and treated groups (n = 5-7 mice per group).

Data are presented as mean ± SEM.

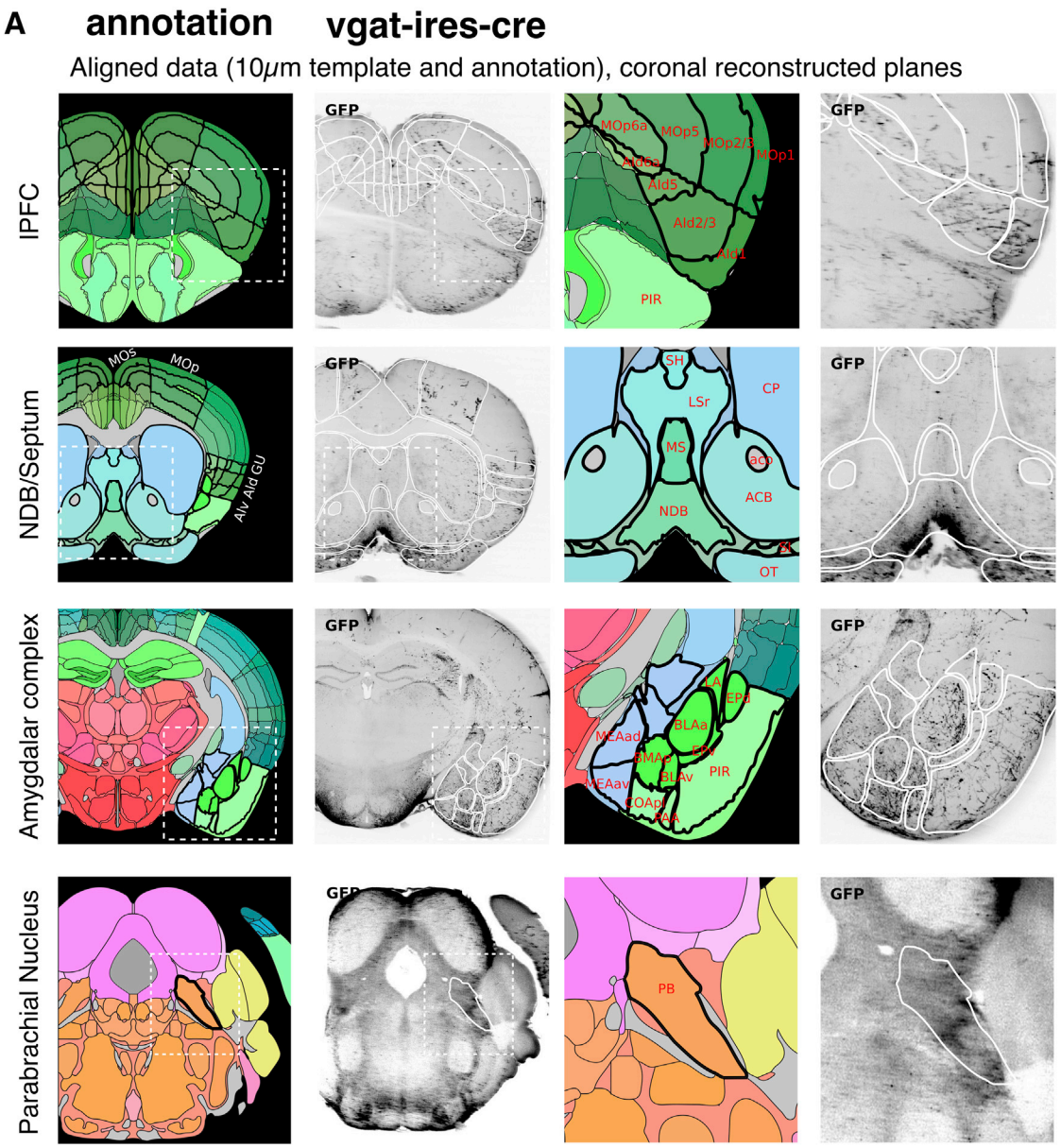

Figure S4. Anterograde Mapping of DRN GABA Circuits, Related to Figure 5

(A) Whole-brain mapping data are displayed for projections to frontal cortex, septum, amygdala, and parabrachial nucleus. Left, broad regional data with inset of region(s) of interest (ROI). Right, magnification of ROI for the aforementioned brain regions.

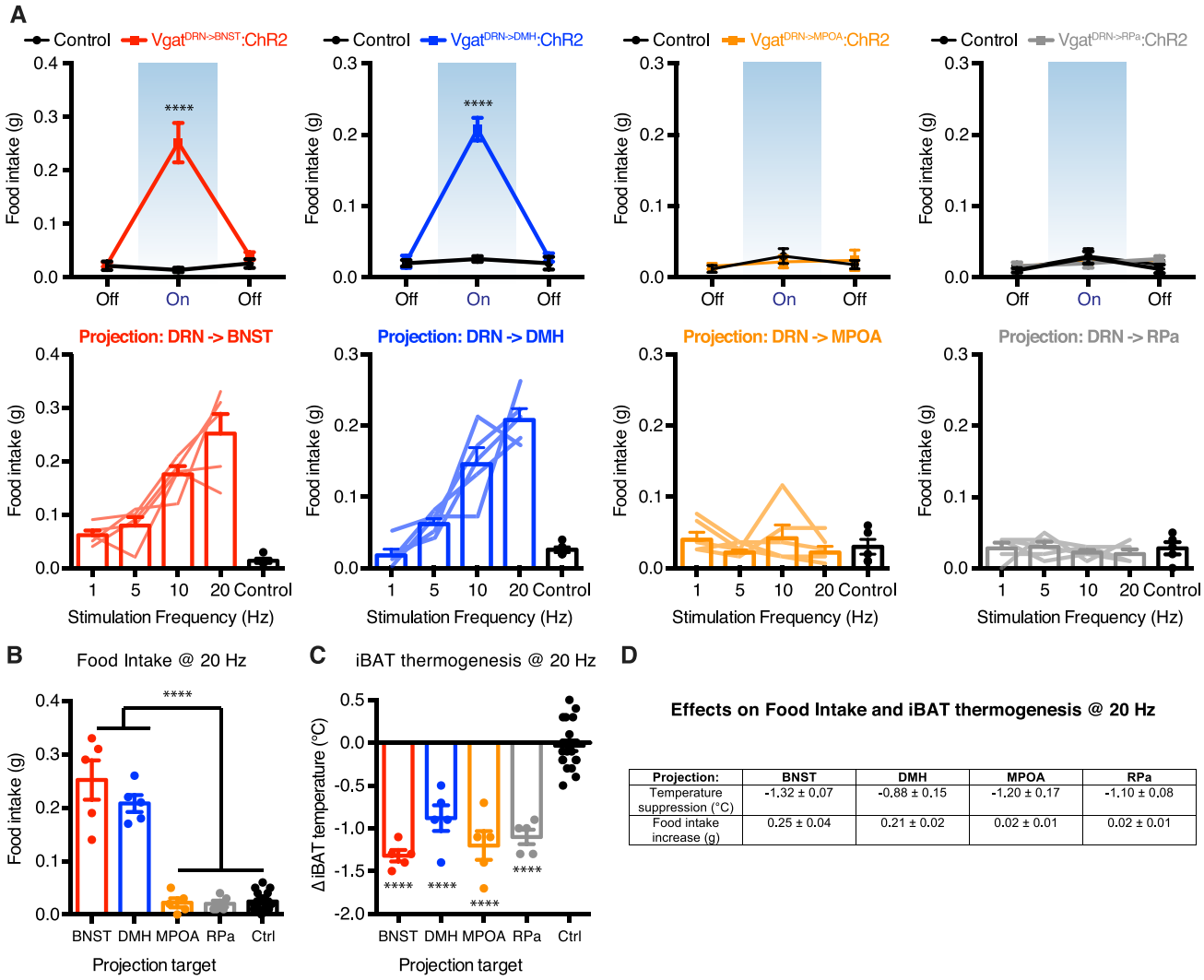

Projection:	BNST	DMH	MPOA	RPa
Temperature suppression (°C)	-1.32 ± 0.07	-0.88 ± 0.15	-1.20 ± 0.17	-1.10 ± 0.08
Food intake increase (g)	0.25 ± 0.04	0.21 ± 0.02	0.02 ± 0.01	0.02 ± 0.01

Figure S5. Projection-Specific Modulation of DRN^{Vgat} Neurons, Related to Figure 7

(A) Activation of DRN^{Vgat} terminals in either the BNST (Treatment: $p < 0.001$) or DMH (Treatment: $p < 0.001$), but not the MPOA (Treatment: $p > 0.05$) or RPa (Treatment: $p > 0.05$), significantly increases food intake (top) in a scalable fashion (bottom). Two-way RM ANOVA comparing control and treated groups (n = 5 mice per group). Blue-shaded region highlights Laser On epoch.

(B) Comparison of food intake increase during photostimulation for DRN^{Vgat} projections to BNST, DMH, MPOA, and RPa. Projection-specific photoactivation significantly augments food intake relative to controls (Treatment: $p < 0.0001$), with differences observed between BNST/DMH and MPOA/RPa treatment groups (BNST/MPOA projections augment food intake, whereas MPOA/RPa projections do not; Treatment: $p < 0.0001$). One-way ANOVA comparing all groups (n = 5-15 mice).

(C) Comparison of iBAT temperature suppression at t = 20 min for projection-specific photoactivation (20 Hz) of DRN^{Vgat} neurons targeting BNST, DMH, MPOA, and RPa (data taken from Figures 6 and 7). Projection-specific photoactivation to these four targets significantly suppresses iBAT temperature relative to controls (Treatment: $p < 0.0001$), with no differences observed between treatment groups ($p > 0.05$). One-way ANOVA comparing all groups (n = 5-15 mice per group).

(D) Table delineating quantitative effects on food intake and iBAT temperature from (B) and (C). All four projections significantly modulate iBAT temperature, whereas only projections to BNST and DMH regulate food intake.

****$p < 0.0001$. Data are presented as mean ± SEM.

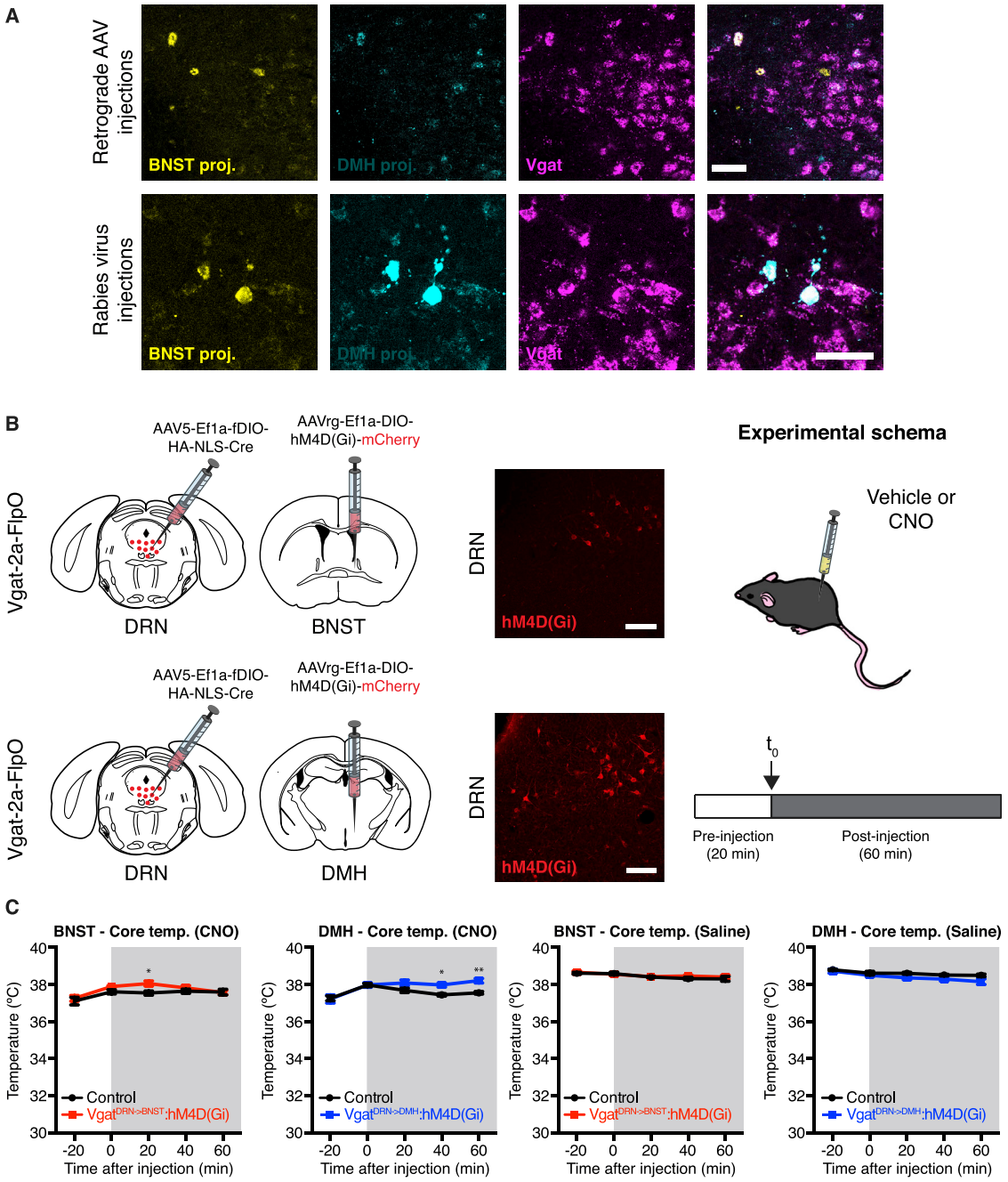

Figure S6. Projection-Specific Inhibition of DRN^{Vgat} Neurons Targeting BNST and DMH, Related to Figure 7

(A) Assessment of collateralization by simultaneous injection of retrograde AAVs (mCherry or EGFP, top) or rabies virus (mCherry or EGFP, bottom) in BNST or DMH. Scale bars, 50 μm.

(B) Strategy and experimental schema for projection-specific inhibition of DRN^{Vgat} neurons projections to BNST or DMH. Vgat-FLPo mice are injected with AAV-EF1a-fDIO-HA-NLS-Cre in the DRN, and AAVrg-EF1a-DIO-hM4D(Gi)-mCherry in the BNST or DMH. Scale bars, 100 μm.

(C) Inhibition of DRN^{Vgat} neurons targeting BNST or DMH transiently elevates core body temperature (left). No effect is observed in saline-injected treated or control mice (right).

*$p < 0.05$, **$p < 0.01$. Data are presented as mean ± SEM.